Monitoring of Molecular Dynamics in Lipid Bilayers of Small Unilamellar Vesicles by Magnetic-Field-Sensitive Probes

Vladimir Ya. Shafirovich,*,† Elena E. Batova,† and Peter P. Levin‡

Contribution from the Institute of Chemical Physics, Russian Academy of Sciences, Chernogolovka 142432, Russia, and Institute of Biochemical Physics, Russian Academy of Sciences, Moscow 117977, Russia

Received November 4, 1994[⊗]

Abstract: In zero magnetic field the recombination of the triplet radical ion pair (RIP) states $^3[P^{\bullet+}-Sp-Vi^{\bullet+}]$ of zinc porphyrin–viologen dyads with the connecting flexible $[(CH_2)_n$, $n = 6, 10]$ or semirigid $[CH_2-(Ph)_m-CH_2$, $m = 1, 2]$ spacers (Sp) between Zn porphyrin (P) and viologen (Vi^{2+}) is a very sensitive analytical tool for detecting the solid–fluid phase transition of the dipalmitoyl (DPPC) or dimyristoyl (DMPC) phosphatidylcholine small unilamellar vesicles. The temperature, $T_m = 33.5-38.5$ °C, and the van't Hoff enthalpy, $\Delta H_{vH} = 80-110$ kcal/mol of the phase transition in DPPC bilayers are compared with those obtained using other techniques. In the fluid membranes (at $T > T_m$) the enhancement of the recombination rates in zero magnetic fields is more pronounced in the case of the flexible $^3[P^{\bullet+}-(CH_2)_n-Vi^{\bullet+}]$ than in the case of the semirigid $^3[P^{\bullet+}-CH_2-(Ph)_m-CH_2-Vi^{\bullet+}]$; the corresponding activation energies are $E_a = 2.7$ and 7.1 kcal/mol ($n = 6$, 10) and 0 and 1.1 kcal/mol ($m = 1$, 2), respectively. The variation of the chain length between the hydrophilic viologen moiety located in the lipid headgroup-water interface and the hydrophobic porphyrin moiety located within the lipid alkyl chains provides for detecting the changes of "microviscosity" in the transversal membrane plane. "Microviscosity" of the DPPC bilayers decreases with the temperature and the distance from the lipid headgroup–water interface; in the temperature range of 42 –70 °C "microviscosities" $\eta = 80-27$ cP ($n = 6$) and 43–5 cP ($n = 10$) are compared with those obtained using other techniques. Application of an external magnetic field ($B \leq 0.21$ T) results in the pronounced retardation of the RIP recombination rates by a factor of 2–11. In a high magnetic field (ca. 0.2 T) the abrupt changes of the recombination rates associated with the phase transitions are not observed; the corresponding $E_a = 0-3.5$ kcal/mol at B = 0.21 T. The magnetic field effects on the recombination rates are discussed in terms of the interplay of spin and chain dynamics modulated by the phase transition and "microviscosity" of phospholipid bilayers.

1. Introduction

A. Kinetic Approach to Detection of Membrane Dynamics. The biological significance of dynamic molecular interactions in natural membranes has stimulated the extensive studies of molecular dynamics in biological and artificial membranes.[1] Membrane dynamics includes molecular motions of different types (translational and rotational). In the kinetic approach to the detection of translational diffusion of molecules in the lateral membrane plane, diffusion coefficients of lateral diffusion are derived from the rates of diffusion-controlled bimolecular processes, particularly the excimer formation,[2] and fluorescence quenching of a probe molecule by paramagnetic ($^3O_2$) and heavy atom (I^-) species,[3] and electron donor[4] and acceptor[5] molecules embedded in membranes. However, difficulties arise due to aggregate formation of the probe molecules[6] caused by the relatively large probe concentrations required to observe the bimolecular processes in phospholipid membranes which have high viscosities. This problem can be solved using the chain-linked bifunctional molecules in which reaction rates are controlled by diffusional encounters of two ends of these molecules. The fascinating effects of membrane dynamics on the end-to-end encounters have been found for instance in dipyrenylalkanes and similar bichromophoric fluorescence probes.[7]

B. Chain-Linked Triplet Radical Ion Pairs as Magnetic-Field-Sensitive Probes of Membrane Dynamics. In the chain-linked triplet biradicals and radical ion pairs (RIPs) the end-to-end reactivity is controlled by spin dynamics which determines

† Institute of Chemical Physics.

‡ Institute of Biochemical Physics.

⊗ Abstract published in *Advance ACS Abstracts*, May 1, 1995.

(1) (a) Yeagle, P. L. *The Structure of Biological Membranes*; CRS Press: Boca Raton, 1992. (b) Gennis, R. B. *Biomembranes: Molecular Structure and Function*; Springer-Verlag: New York, 1989. (c) Eddin, E. In *Membrane Structure*; Finean, J. B., Michell, R. H., Eds.; Elsevier: Amsterdam, 1981.

(2) (a) Vanderkooi, J. M.; Callis, J. B. *Biochemistry* **1974**, *13*, 4000. (b) Galla, H.-J.; Sackmann, E. *Biochem. Biophys. Acta* **1974**, *339*, 103. (c) Vanderkooi, J. M.; Fischkoff, S.; Andrich, M.; Podo, F.; Owen. *J. Chem. Phys.* **1975**, *63*, 3661. (d) Emert, J.; Behrens, C.; Merrill, G. *J. Am. Chem. Soc.* **1979**, *101*, 771. (e) Tanaka, F.; Kaneda, N.; Mataga, N. *J. Am. Chem. Soc.* **1986**, *90*, 3167. (f) Pansu, R. B.; Yoshihara, K.; Arai, T.; Tokumaru, K. *J. Phys. Chem.* **1993**, *97*, 1125.

(3) (a) Bohorguez, M.; Patterson, L. K. *J. Phys. Chem.* **1988**, *92*, 1835. (b) Caruso, F.; Grieser, F.; Tristlethwaite, P.; Almgren, M.; Wistus, E.; Mukhtar, E. *J. Phys. Chem.* **1993**, *97*, 7364.

(4) (a) Kano, K.; Kawazumi, H.; Ogawa, T.; Sunamoto, J. *J. Phys. Chem.* **1981**, *85*, 2204. (b) Caruso, F.; Grieser, F.; Murphy, A.; Tristlethwaite, P.; Urquhart, R.; Almgren, M.; Wistus, E. *J. Am. Chem. Soc.* **1991**, *113*, 4838.

(5) (a) Chance, B.; Erecinska, M.; Radda, G. *Eur. J. Biochem.* **1975**, *54*, 521. (b) Fato, R.; Battino, M.; Castelli, G. P.; Lenaz, G. *FEBS Lett.* **1985**, *179*, 238. (c) Fato, R.; Battino, M.; Delgi Esposti, M.; Castelli, G. P.; Lenaz, G. *Biochemistry* **1986**, *25*, 3378. (d) Lemmetyinen, H.; Yliperttula, M.; Mikkola, J.; Kinnunen, P. *Biophys. J.* **1989**, *55*, 885.

(6) (a) Brocklehurst, J. R.; Freedman, R. B.; Hancock, D. J.; Radda, G. K. *Biochem. J.* **1970**, *116*, 721. (b) Somerharju, P. J.; Virtanen, J. A.; Eklund, K. E.; Vainio, P.; Kinnunen, P. K. J. *Biochemistry* **1985**, *24*, 2773. (c) Blackwell, M. F.; Gounaris, K.; Barber, J. *Biochem. Biophys. Acta* **1986**, *858*, 221. (d) Lemmetyinen, H.; Yliperttula, M.; Mikkola, J.; Virtanen, J. A.; Kinnunen, P. K. J. *J. Phys. Chem.* **1989**, *93*, 7170.

(7) (a) Zachariasse, K. A.; Kühnle, W.; Weller, A. *Chem. Phys. Lett.* **1980**, *73*, 6. (b) Georgescauld, D.; Desmasez, J. P.; Lapouyade, R.; Babeau. A.; Richard, H.; Winnik, M. *Photochem. Photobiol.* **1980**, *31*, 539. (c) Melnick, R. L.; Haspel, H. C.; Goldenberg, M.; Greenbaum, L. M.; Weinstein, S. *Biochem. J.* **1981**, *34*, 499. (d) Zachariasse, K. A. In *Fluorescence Techniques and Membrane Markers in Cancer and Immunology: Membrane Dynamics, Cellular Characterization and Cell Sorter*; Viallet, P., Ed.; Elsevier: Amsterdam, 1984.

0002-7863/95/1517-6093$09.00/0

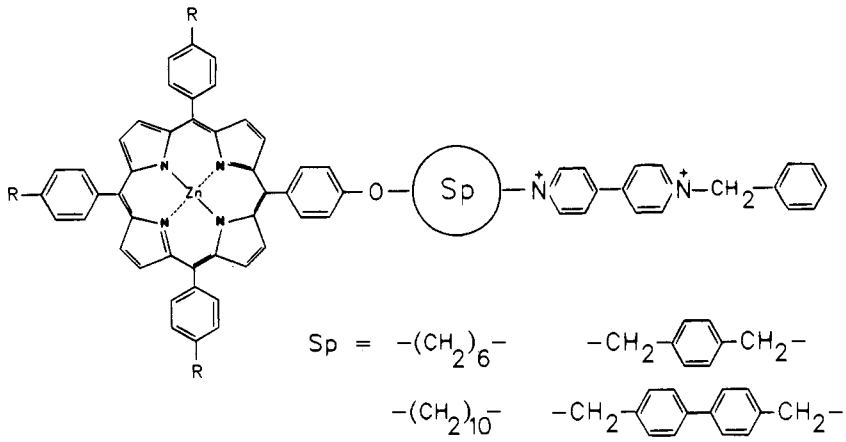

Figure 1. Molecular structure of the P−Sp−Vi^{2+} dyads.

spin realignment required for formation of diamagnetic products. Interplay of chain and spin dynamics provides the intriguing magnetic field, solvent viscosity, and temperature effects on the recombination rates of the triplet biradicals and RIPs.[8] The salient feature of the solvent viscosity and temperature effects on the recombination rate constant $k_r(B)$ is that these effects are strikingly dependent on the magnetic field strength B. In membranes random chain motions, and hence the recombination rates of probe triplet RIPs, can be modulated by dynamics of phospholipid bilayers. Our preliminary studies have shown[9] that in zero magnetic field the solid−fluid phase transitions in membranes of the small unilamellar vesicles exhibit the pronounced effects on the $k_r(B=0)$ values of the semirigid zinc porphyrin−viologen triplet RIPs. The phase transition effects on the recombination rates disappeared in high magnetic fields.

In this paper we extended using the magnetic-field-sensitive recombination of the triplet RIPs to probing membrane dynamics, particularly for monitoring "microviscosity" in the small unilamellar vesicles. Four P−Sp−Vi^{2+} dyads[10] (Figure 1) with the connecting flexible [$(CH_2)_n$, n = 6, 10] or semirigid [CH_2−$(Ph)_m$−CH_2, m = 1, 2] spacers (Sp) were used in these studies. The corresponding flexible and semirigid spacers are approximately the same length but have different rigidities, and hence these dyads are excellent candidates for testifying the effects of the RIP intramolecular mobility on the recombination kinetics. Here, we show that in zero magnetic field the flexible $^3[P^{\bullet+}-(CH_2)_n-Vi^{\bullet+}]$ are more sensitive to the temperature changes of membrane dynamics and can be used not only for detecting the phase transitions as the semirigid $^3[P^{\bullet+}-CH_2-(Ph)_m-CH_2-Vi^{\bullet+}]$ but also *for monitoring the "microviscosity"* (η) of the fluid vesicular membranes. The estimates of the η values were obtained by comparing the $k_r(B=0)$ values measured in the vesicular membranes with those obtained in the methanol−glycerol mixtures of known η. For diagnostics of the spin dynamics mechanisms we used the magnetic field effect[8] on the recombination kinetics of the triplet RIPs.

2. Experimental Section

The dyads containing PF_6^- as a counter anion were prepared and purified by the methods described previously.[10d] The spectroscopic data of the dyads synthesized were consistent with the assigned structures. D,L-Dipalmitoyl-α-phosphatidylcholine and D,L-dimyristoyl-α-phosphatidylcholine from Fluka (Bucks, Switzerland) were used without further purification. Other chemicals were the best available grade from commercial supplies. Water was triply distilled.

The small unilamellar vesicles were prepared by the methods described previously.[9] Lipid (12.5 μM) and the dyad (0.08 μM) were mixed in 3 mL of methanol−benzene (1:1). The solvent was evaporated under a stream of argon leaving a film of the lipid on the surface of a glass tube. The lipid film was dried under vacuum and then suspended in 2.5 mL of 0.04 M phosphate buffer aqueous solution (pH 6.5). The sample was sonicated for 25 min at 50−60 °C under a stream of argon and then centrifuged at 8000 g for 20 min. The dyad concentration in phospholipid bilayers was equal to ~0.6 mol %. The freshly prepared vesicle dispersions were used throughout this work. In these dispersions a fraction of the small unilamellar vesicles determined by gel chromatography[11] at Sepharose 2B was greater than 80−90%. Electron microscope determinations using negative staining showed that the majority of the sonicated vesicles had a diameter between 200 and 300 Å.[12]

The absorption spectra and decay kinetics of the intermediates were recorded by nanosecond laser flash photolysis using a PRA LN-102 dye laser (420 nm) pumped by an LN-1000 nitrogen laser as an excitation source.[13] Kinetic curves were averaged over 128 laser pulses by a Biomation 6500 waveform recorder coupled to an Apple IIe microcomputer. Each kinetic curve was recorded at 1024 points with 2, 5, 10, and 20 ns per point. A total of ≥800 points in the time interval covering nearly 100% of the amplitude change was used for analysis of the experimental kinetic curves by the sum of several exponents. The fitting procedure was a nonlinear least-squares method using the Marquardt algorithm. The quality of fitting was judged by the residuals and autocorrelation as well as by the standard deviation and the statistical parameter Durbin Watson. The data presented are the average of the results based on calculations performed on at least five kinetic curves obtained for a given temperature and external magnetic field.

In the magnetic field experiments a 1-cm quartz cell with a water jacket kept at 5−70 °C was placed between two pole pieces of a permanent magnet. By changing the distance between the pole pieces, B can be varied from 0 to 0.21 T. Before the laser photolysis studies the cell was carefully evacuated on a vacuum pump line up to 0.1 Pa (ca. 10^{-3} Torr) and filled with argon. In order to get the temperature profiles of $k_r(B)$ the sample was cooled at first from room temperature to 5 °C and then heated to selected temperatures at the rate of 0.5 °C/

(8) For recent reviews see: (a) Doubleday, C., Jr.; Turro, N. J.; Wang, J.-F. *Acc. Chem. Res.* **1989**, *22*, 199. (b) Steiner, U. E.; Ulrich, T. *Chem. Rev.* **1989**, *89*, 51. (c) Steiner, U. E.; Wolff, H.-J. In *Photochemistry and Photophysics*; Rabek, J. F., Scott, G. W., Eds.; CRS Press: Boca Raton, 1991; Vol. 4. (d) Khudyakov, I. V.; Serebrennikov, Yu. A.; Turro, N. J. *Chem. Rev.* **1993**, *93*, 537.

(9) Shafirovich, V. Ya.; Batova, E. E.; Levin, P. P. *Photochem. Photobiol.* **1992**, *55*, 473.

(10) (a) Levin, P. P.; Batova, E. E.; Shafirovich, V. Ya. *Chem. Phys.* **1990**, *142*, 279. (b) Shafirovich, V. Ya.; Batova, E. E.; Levin, P. P. *Chem. Phys. Lett.* **1992**, *172*, 10. (c) Shafirovich, V. Ya.; Batova, E. E.; Levin, P. P. *Chem. Phys.* **1992**, *162*, 155. (d) Shafirovich, V. Ya.; Batova, E. E.; Levin, P. P. *J. Chem. Soc., Faraday Trans.* **1992**, *88*, 935.

(11) Huang, C. *Biochemistry* **1969**, *8*, 344.

(12) Maier, V. E.; Levchenko, L. A.; Shafirovich, V. Ya. *Kinet. Katal.* **1986**, *27*, 1378.

(13) Levin, P. P.; Pluzhnikov, P. F.; Kuzmin, V. A. *Chem. Phys. Lett.* **1988**, *147*, 283.

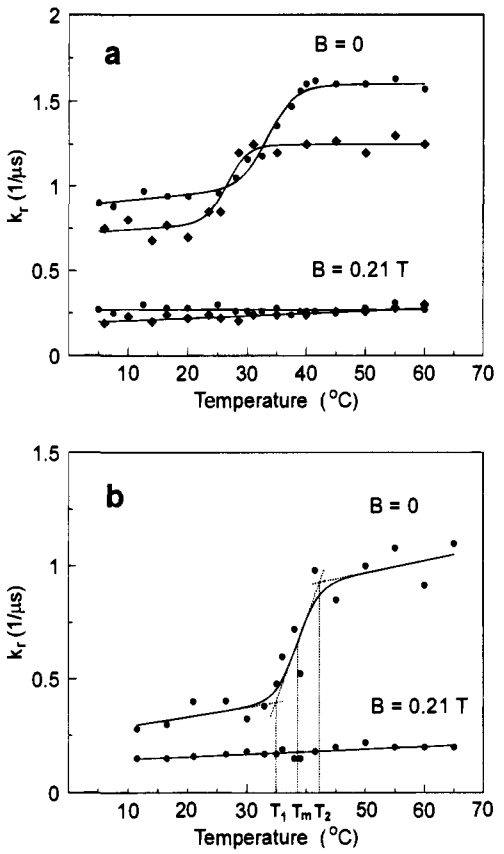

Figure 2. The temperature profiles of the recombination rate constant k_r of $^3[P^{\bullet+}-CH_2-Ph-CH_2-Vi^{\bullet+}]$ (a) and $^3[P^{\bullet+}-CH_2-Ph-Ph-CH_2-Vi^{\bullet+}]$ (b) in the DPPC (●) and DMPC (◆) small unilamellar vesicles. The solid lines representing the fits of eq 5 (B = 0) and the Arrhenius eq (B = 0.21 T) with the parameters from Table 1 are superimposed on the experimental points (●, ◆). The errors in determination of k_r do not exceed ±5−10% in the fluid ($T > T_2$) and solid ($T < T_1$) phases and ±10−15% in the range of phase transition ($T_1 < T < T_2$). The values of k_r for $^3[P^{\bullet+}-CH_2-Ph-CH_2-Vi^{\bullet+}]$ in DPPC vesicles were taken from ref 9.

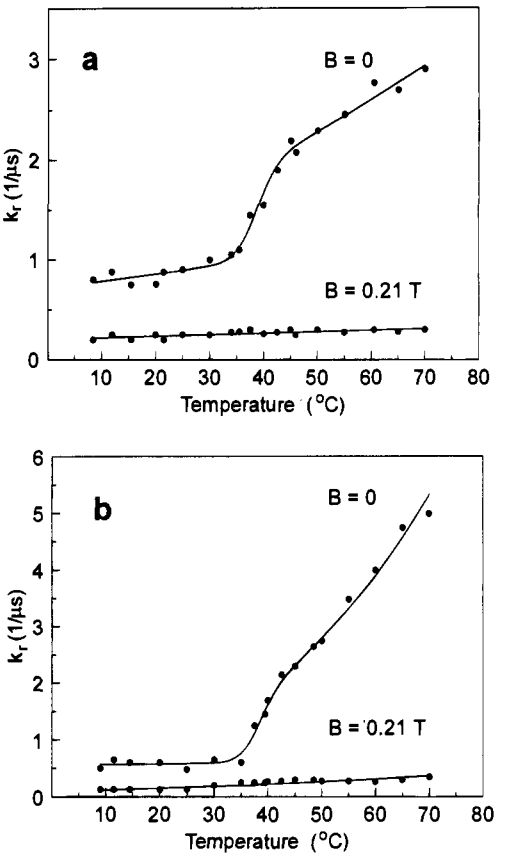

Figure 3. The temperature profiles of the recombination rate constant k_r of $^3[P^{\bullet+}-(CH_2)_6-Vi^{\bullet+}]$ (a) and $^3[P^{\bullet+}-(CH_2)_{10}-Vi^{\bullet+}]$ (b) in the DPPC small unilamellar vesicles. The solid lines representing the fits of eq 5 (B = 0) and the Arrhenius eq (B = 0.21 T) with the parameters from Table 1 are superimposed on the experimental points (●). The errors in determination of k_r do not exceed ±5−10% in the fluid ($T > T_2$) and solid ($T < T_1$) phases and ±10−15% in the range of phase transition ($T_1 < T < T_2$).

min by using a circulating water bath with a temperature programmer. Before measurements the temperature equilibration within the cell was established by equilibrating the sample for ca. 10 min at these temperatures.

3. Results

3.1. General Aspects. Effects of Temperature on Magnetic-Field-Sensitive Recombination of $^3[P^{\bullet+}-Sp-Vi^{\bullet+}]$ in Vesicular Membranes. Laser photoexcitation of $P-Sp-Vi^{2+}$ embedded in phospholipid bilayers of small unilamellar vesicles results in the appearance of the triplet excited, $^3P-Sp-Vi^{2+}$ (a shoulder at 470 nm), and radical ion pair, $P^{\bullet+}-Sp-Vi^{\bullet+}$ (λ_{max}= 620 nm), states; the characteristic transient absorption spectra are close to those in organic solvents.[10] The transient absorption decays are comprised of a fast component (k_e), which correspond to the intramolecular quenching of ^3P by Vi^{2+} (absorption decay at 470 nm) accompanied by triplet RIP formation (absorption rise at 620 nm) and a slow component (k_r) reflecting the RIP decay (absorption decay at 470 and 620 nm).[9,10] Depending on the temperature, dyad structure, and phase state of lipid bilayers the values of k_e are varied in the (5−20) × 10^6 s^{-1} range, which is greater than the corresponding k_r values.

The effects of temperature on the RIP recombination rate constant $k_r(B)$ depend on the magnetic field strength B. Figures 2 and 3 show that $k_r(B$=0) are greater than $k_r(B$=0.21T) and exhibit the single abrupt changes associated with the solid-fluid phase transitions of vesicular membranes.[14] In the solid phase (before the phase transition, i.e. at $T < T_1$, see Figure 2b) the activation energies, E_s, obtained in zero magnetic field (see section 3.2) do not exceed ca. 2 kcal/mol and exhibit no correlation with the spacer length and rigidity (Table 1). The striking effect of the spacer structure on the activation energies, E_f, measured in zero magnetic field (see section 3.2) is observed in the fluid state (after the phase transition, i.e. at $T > T_2$, see Figure 2b). The E_f values of the flexible RIPs are greater than those of the corresponding semirigid RIPs and increase with spacer length (Table 1). The temperature profiles of $k_r(B$=0) for the flexible RIPs were used in the estimates of "microviscosities" in the fluid membranes (see section 3.3). In the strong magnetic field the abrupt changes of $k_r(B$=0.21T) associated with the solid−fluid phase transitions are not observed (Figures 2 and 3) and the activation energies, $E_a(B$=0.21T), do not exceed ca. 3.5 kcal/mol (Table 1).

Figure 4 shows the typical magnetic field dependencies of $k_r(B)$ for the flexible $^3[P^{\bullet+}-(CH_2)_n-Vi^{\bullet+}]$ in the fluid vesicular membranes. These dependencies can be characterized by the following parameters: B_{max}, the magnetic field strength at which

(14) (a) Sheetz, M. P.; Chan, S. E. *Biochemistry* **1972**, *11*, 4573. (b) Suurkuusk, J.; Lentz, B. R.; Barenholz, Y.; Biltonen, R.; Thompson, T. E. *Biochemistry* **1976**, *15*, 1393. (c) Lentz, B. R.; Barenholz, Y.; Thompson, T. E. *Biochemistry* **1976**, *15*, 4521.

Table 1. Phase Transition Parameters of the DPPC Small Unilamellar Vesicles Estimated from the Recombination Rates of the Triplet Radical Ion Pairs[a]

triplet RIP	T_m (°C)	ΔH_{vH} (kcal/mol)	E_s[d] (kcal/mol)	E_f[d] (kcal/mol)	E_a (B=0.21T)[d] (kcal/mol)
$^3[P^{\bullet+}-CH_2-Ph-CH_2-Vi^{\bullet+}]$[b]	33.5	80	0.6	0	0
$^3[P^{\bullet+}-CH_2-Ph-CH_2-Vi^{\bullet+}]$[c]	26.5	100	0.5	0	1.1
$^3[P^{\bullet+}-CH_2-Ph-Ph-CH_2-Vi^{\bullet+}]$	38.5	110	2.1	1.1	1.2
$^3[P^{\bullet+}-(CH_2)_6-Vi^{\bullet+}]$	38.5	100	1.5	2.7	1.1
$^3[P^{\bullet+}-(CH_2)_{10}-Vi^{\bullet+}]$	38	105	0.3	7.1	3.5

[a] The error in determination of T_m does not exceed ±5%; and the errors of ΔH_{vH}, E_s, E_f, and E_a(B=0.21T) in most cases do not exceed ±20%. [b] Calculated from data of ref 9. [c] DMPC small unilamellar vesicles. [d] The corresponding values of $k_{rs}°$, $k_{rs}°$, and $k_r°$(B=0.21T) are given in Table 2 (see, supplementary material).

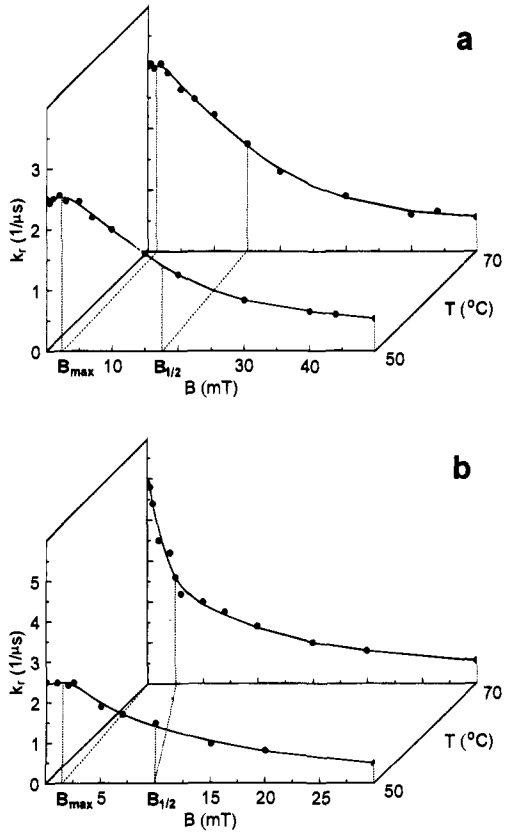

Figure 4. The effects of temperature on the magnetic field dependences of the recombination rate constant k_r of $^3[P^{\bullet+}-(CH_2)_6-Vi^{\bullet+}]$ (a) and $^3[P^{\bullet+}-(CH_2)_{10}-Vi^{\bullet+}]$ (b) in the DPPC small unilamellar vesicles. The errors in determination of k_r do not exceed ±5−10%.

k_r(B) exhibit a maximum,[15] and $B_{1/2}$, the magnetic field strength at which $k_r(B) = [k_r(B=0) - k_r(B=0.21T)]/2$. The reduction of the $k_r(B=0)$ values with a decrease in the temperature correlates with the shifts of B_{max} and $B_{1/2}$ in high fields (Figure 4). In the case of the semirigid $^3[P^{\bullet+}-CH_2-Ph-CH_2-Vi^{\bullet+}]$ the temperature effects on B_{max} and $B_{1/2}$ were not observed.[9]

3.2. Phase Transition Parameters of Vesicular Membranes. The temperature profiles of $k_r(B=0)$ (see, Figures 2 and 3) were analyzed in terms of the averaged rate constant[20] expressed by the following equation

$$k_r = A_s k_{rs} + A_f k_{rf} \quad (1)$$

where A_s and A_f are the mole fractions of the solid and fluid phases, and k_{rs} and k_{rf} are the recombination rate constants in these phases. The temperature dependencies of k_{rs} and k_{rf} were described by the Arrhenius equation

$$k_{rs} = k_{rs}° \exp(-E_s/RT) \quad (2)$$

$$k_{rf} = k_{rf}° \exp(-E_f/RT) \quad (3)$$

where E_s and E_f are the corresponding activation energies. The solid−fluid transition was considered as a two-state reaction; the equilibrium constant for this reaction was calculated by the van't Hoff equation

$$K = A_f/A_s = \exp[-(\Delta H_{vH}/RT - \Delta H_{vH}/RT_m)] \quad (4)$$

where ΔH_{vH} is the apparent transition enthalpy[21] (the so-called van't Hoff enthalpy) and T_m is the temperature of the phase transition (Figure 2b) which can be defined as the temperature that corresponds to the maximum of the first derivative of the $k_r(T)$ function. Combination of eqs 1−4 leads to the following equation for the RIP recombination rates

$$k_r = k_{rf}° \exp(-E_f/RT) + [k_{rs}° \exp(-E_s/RT) - k_{rf}° \exp(-Ef/RT)] \exp[-(\Delta H_{vH}/RT - \Delta H_{vH}/RT_m)]/\{1 + \exp[-(\Delta H_{vH}/RT - \Delta H_{vH}/RT_m)]\} \quad (5)$$

Figures 2 and 3 show the most satisfactory fits of eq 5 to the experimental plots of $k_r(B=0)$ vs temperature.

Phase transition parameters for the DPPC and DMPC small unilamellar vesicles obtained in the fitting procedure are summarized in Table 1. The T_m values of the DPPC vesicles are greater than those of the DMPC vesicles. For the DPPC vesicles the values of T_m = 38.0−38.5 °C do not depend on the spacer length and rigidity of the probe molecules, and only in the case of $^3[P^{\bullet+}-CH_2-Ph-CH_2-Vi^{\bullet+}]$ is the value of T_m somewhat less (T_m = 33.5 °C). The obtained values of ΔH_{vH} are in the range of 80−110 kcal/mol and do not exhibit a certain correlation with the structures of the lipid and probe molecules.

(15) Magnetic field dependencies with a local maximum were first observed for biradical-derived CIDNP[16] and more recently for the pyrene triplet yields in non-linked pyrene−dimethylaniline systems[17] and recombination rates[18] of flexible triplet biradicals. On many occasions[9,10,19] increasing the recombination rates with B was not so pronounced and the corresponding magnetic field curves exhibit an "initial" plateau rather than a local maximum; in this case B_{max} is taken as a middle point of the initial plateau.

(16) (a) Closs, G. L.; Doubleday, C., Jr. *J. Am. Chem. Soc.* **1973**, *95*, 2735. (b) Closs, G. L. *Adv. Magn. Reson.* **1975**, *7*, 1.

(17) (a) Weller, A.; Staerk, H.; Treichel, R. *Faraday Discuss. Chem. Soc.* **1984**, *78*, 271. (b) Staerk, H.; Kuhnle, W.; Treichel, R.; Weller, A. *Chem. Phys. Lett.* **1985**, *118*, 19.

(18) (a) Zimmt, M.; Doubleday, C., Jr.; Turro, N. J. *J. Am. Chem. Soc.* **1985**, *107*, 6726. (b) Wang, J.; Doubleday, C., Jr.; Turro, N. J. *J. Phys. Chem.* **1989**, *93*, 4780.

(19) (a) Shafirovich, V. Ya.; Batova, E. E.; Levin, P. P. *J. Phys. Chem.* **1993**, *97*, 4877. (b) Shafirovich, V. Ya.; Batova, E. E.; Levin, P. P. Z. *Phys. Chem.* **1993**, *182*, 245.

(20) In the temperature range (T_1 − T_2) of the phase transition (Figure 2B) in which the solid and fluid phase coexist, a biexponential form, $A_f \exp(-k_{rf}t) + A_s \exp(-k_{rs}t)$, of the RIP decay is expected rather than a monoexponential one. However, in this work we did not get unambiguous fits in terms of a biexponential decay because the k_{rf} and k_{rs} values differ only by a factor of ~2 (Figures 2 and 3), and signal/noise ratio is not so high.

(21) (a) Sturtevant, J. M. *Annu. Rev. Biophys. Bioeng.* **1974**, *3*, 35. (b) Lee, A. G. *Prog. Biophys. Mol. Biol.* **1975**, *29*, 3.

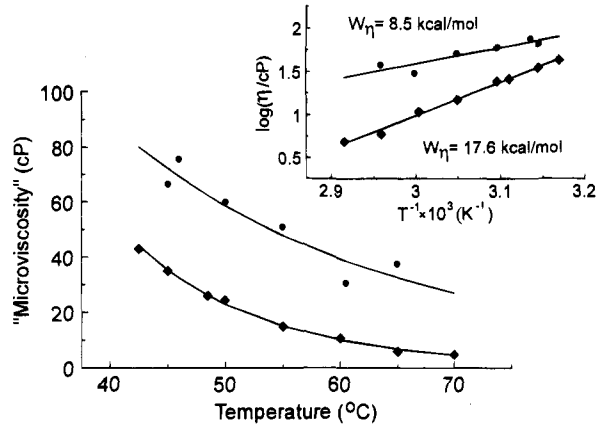

Figure 5. The effects of temperature on the "microviscosity" η of the DPPC small unilamellar vesicles obtained comparing the recombination rate constant $k_r(B=0)$ of $^3[P^{\bullet+}-(CH_2)_6-Vi^{\bullet+}]$ (●) and $^3[P^{\bullet+}-(CH_2)_{10}-Vi^{\bullet+}]$ (◆) in vesicular membranes and in the methanol–glycerol mixtures whose viscosities were measured.[19a] The solid lines representing the fits of eq 6 with the parameters from Table 2 (see, Supplementary Materials) are superimposed on the experimental points (●, ◆). The "microviscosity" determination error ±10–20%.

3.3. "Microviscosity" of Fluid Vesicular Membranes. The values of "microviscosity" were obtained by comparing the $k_r(B=0)$ values of the flexible RIPs recorded in vesicular membranes (Figure 3) with those[19a] measured in methanol–glycerol mixtures with known η.

The solid phases of vesicular membranes are characterized by extremely high "microviscosities", and the $k_r(B=0)$ values of the flexible RIPs (Figure 3) give a low limit of $\eta > 1300$ cP only because these values are less than those in pure glycerol (1300 cP), which is the most viscous medium used.[19b]

In the fluid bilayers (45–70 °C) the $k_r(B=0)$ values of $^3[P^{\bullet+}-(CH_2)_n-Vi^{\bullet+}]$ (Figure 3) are comparable with those[19a] in the methanol–glycerol mixtures (80–30 cP for $n = 6$ and 45–5 cP for $n = 10$) and give a measure of the bilayer "microviscosities". By using the relationship between $k_r(B=0)$ and η of the methanol–glycerol mixtures,[19a] the temperature profiles of $k_r(B=0)$ for the flexible RIPs (Figure 3) were recalculated into the η vs temperature plots. Figure 5 shows that the bilayer "microviscosties" estimated by this method depend on a spacer length, and $^3[P^{\bullet+}-(CH_2)_{10}-Vi^{\bullet+}]$ exhibits lower values of η than $^3[P^{\bullet+}-(CH_2)_6-Vi^{\bullet+}]$ by a factor of 2–3. The temperature profiles of η were described by the following equation:[22]

$$\eta = \eta^\circ \exp(W_\eta/RT) \qquad (6)$$

where W_η is the "microactivation" energy of viscous flow in vesicular membranes. The most satisfactory fits of eq 6 to the experimental plots of η vs temperature were obtained at W_η = 8.5 and 17.6 kcal/mol for $^3[P^{\bullet+}-(CH_2)_6-Vi^{\bullet+}]$ and $^3[P^{\bullet+}-(CH_2)_{10}-Vi^{\bullet+}]$, respectively (Figure 5).

4. Discussion

4.1. Interplay of Chain and Spin Dynamics in $^3[P^{\bullet+}-Sp-Vi^{\bullet+}]$ Embedded in Vesicular Membranes. The overall end-to-end reactivity of the chain-linked triplet biradicals and RIPs can be considered in terms of the kinetic approach developed by Closs, Forbes, and co-workers.[23] In the absence of the applied magnetic fields the electron-nuclear hyperfine coupling (hfc) induces efficient mixing between the triplet (T) and singlet (S) manifolds in the extended conformations of the radical pair in which the exchange interaction (J) between unpaired electrons is small compared to hfc. With a non-zero J, the triplet-derived states acquire a certain degree of singlet character, λ. Multiplying this singlet character with the end-to-end encounter rate constant k_{en} gives the rate constant $k_{en}\lambda$ for the exit to diamagnetic products. The T–S mixing also occurs by nuclear spin independent processes, mostly by the spin–orbit coupling (SOC).[24] The efficiency of SOC rapidly decreases with the end-to-end distance in the pair,[8] and the pure singlet states produced by SOC in the folded conformations of the radical pair undergo a prompt chemical reaction.[25b] Therefore, the return of the S state to any T level by this mechanism can be ignored and adding a term k_{SOC} to $k_{en}\lambda$ gives the total rate constant.[23]

In a strong magnetic field SOC provides a unique pathway for the recombination of radical pairs in $T_\pm$ states, because the hfc and relaxation routes of $T_\pm-T_0,S_0$ transitions in radical pairs are suppressed.[8] In support of this mechanism, we found the pronounced external heavy-atom effect on the $B = 0.21$T values for the recombination of $^3[P^{\bullet+}-CH_2-Ph-CH_2-Vi^{\bullet+}]$ in CTAC/CTAB micelles.[10b] In the case of $^3[P^{\bullet+}-Sp-Vi^{\bullet+}]$ the values of k_{SOC} are significantly less than the values of k_{en}, which explains the very small viscosity effects on the $k_r(B=0.21T)$ values.[10c,19] Since k_{SOC} is expected to be independent of temperature,[8] it is not surprising that the values of $k_r(B=0.21T)$ are also only weakly dependent on temperature (Figures 2 and 3). The small positive values of $E_a(B=0.21T)$ for the $^3[P^{\bullet+}-Sp-Vi^{\bullet+}]$ recombination in vesicular membranes (Table 1) are close to those in isotropic fluids.[10a,d] Turro and co-workers[26] have reported similar values of E_a for the recombination of the short flexible dibenzylic triplet biradicals for which the T–S mixing induced by SOC dominates.

The effects of chain dynamics on the encounter rate constant are straightforward, the smaller jump frequencies of the connecting polymethylene chains due to increasing the viscosity or decreasing the temperature result in smaller k_{en}.[27] These effects dominate at low temperatures and high viscosities and manifest themselves by positive activation energies in the low-temperature recombination of the long-chain-linked acyl–benzyl[26] and xanthone ketyl–xanthenyl[28] triplet biradicals, as well as the retardation of the recombinination of $^3[P^{\bullet+}-(CH_2)_n-Vi^{\bullet+}]$ in viscous media.[19a] In vesicular membranes which can be considered as viscous two-dimentional liquids,[1,2a,c] the abrupt decrease in the membrane "microviscosities" associated with the solid–fluid phase transitions of vesicular membranes[14] seems to be responsible for the corresponding increase in the $k_r(B=0)$ values (Figures 2 and 3). In the case of flexible $^3[P^{\bullet+}-(CH_2)_n-Vi^{\bullet+}]$, comparing the $k_r(B=0)$ values in the fluid membranes (Figure 3) with those in methanol–glycerol mixtures[19a] gives the plausible values of the membrane "microviscosities" (see Figure 5 and section 4.3).

The effects of chain dynamics on the singlet character are mostly related to the modulation of the hfc-induced T–S mixing due to the J variations induced by the random folding and

(22) Alwattar, A. H.; Lumb, M. D.; Birks, J. B. In *Organic Molecular Photophysics 1*; Birks, J. B., Ed.; Willey: New York, 1973; Vol. 1, p 403.

(23) (b) Closs, G. L.; Forbes, M. D. E. *J. Phys. Chem. Soc.* **1991**, *95*, 1924. (b) Closs, G. L.; Forbes, M. D. E.; Piotrowiak, P. *J. Am. Chem. Soc.* **1992**, *114*, 3285.

(24) It is well-known that SOC is the dominant mechanism in some acyl–alkyl triplet biradicals.[25]

(25) (a) Closs, G. L. In *Chemically Induced Magnetic Polarization*; Muus, L. T., Atkins, P. W., McLauchlan, K. A., Pedersen, J. B., Eds.; Reidel: Dordrecht, Holland, 1977. (b) DeKanter, F. J. J.; Kaptein, R. *J. Am. Chem. Soc.* **1982**, *104*, 4759.

(26) (a) Wang, J.-P.; Doubleday, C., Jr.; Turro, N. J. *J. Am. Chem. Soc.* **1989**, *111*, 3962. (b) Zimmt, M.; Doubleday, C., Jr.; Turro, N. J. *J. Am. Chem. Soc.* **1986**, *108*, 3618.

(27) For reviews see: (a) Winnik, M. *Chem. Rev.* **1981**, *81*, 491. (b) Winnik, M. *Acc. Chem. Res.* **1985**, *18*, 73.

(28) Tanomoto, Y.; Samejima, N.; Tamura, T.; Hayashi, M. *Chem. Phys. Lett.* **1992**, *188*, 446.

torsional motions of the polymethylene chains.[29] The theoretical treatment of Schulten and Bittl[32] and extensive computer simulations of Staerk and co-workers[33] have shown that decreasing the jump frequencies reduces the effective exchange interaction (J_{eff}). The J_{eff} reduction enhances the hfc-induced T−S mixing, which in turn increases the recombination rates. This effect seems to be very surprising in classical kinetics (without spin) because the slower jump frequencies result in the faster recombination rates.[34] For instance, the chain-linked benzyl−benzyl[26] and xanthone ketyl−xanthenyl[28] triplet biradicals exhibit negative activation energies in the high-temperature recombination, and $^3[P^{\bullet+}-(CH_2)_6-Vi^{\bullet+}]$[19a] shows the enhancement of $k_r(B=0)$ at low viscosities (0.5−30 cP). Chain dynamics in semirigid $^3[P^{\bullet+}-CH_2-Ph-CH_2-Vi^{\bullet+}]$ is strikingly unlike that in $^3[P^{\bullet+}-(CH_2)_6-Vi^{\bullet+}]$ with a flexible spacer of approximately the same length; the $k_r(B=0)$ values monotonously increase[19b] in a wider viscosity range (0.5−1300 cP). Hence, in vesicular membranes a reduction of $k_r(B=0)$ with tempearture can be most likely expected for $^3[P^{\bullet+}-CH_2-Ph-CH_2-Vi^{\bullet+}]$ instead of an enhancement of $k_r(B=0)$ observed for $^3[P^{\bullet+}-(CH_2)_n-Vi^{\bullet+}]$ (see Figure 2). However, this effect has not been found in viscous anisotropic fluids; the $k_r(B=0)$ values of $^3[P^{\bullet+}-CH_2-Ph-CH_2-Vi^{\bullet+}]$ in the fluid vesicular membranes (η = 5−80 cP, Figure 5) and in the micelles[10b] (e.g., η = 33−39 cP in CTAB micelles[35]) are close to those in nonviscous organic solvents.[10a,c] The absence of the correlation between the $k_r(B=0)$ values of $^3[P^{\bullet+}-CH_2-Ph-CH_2-Vi^{\bullet+}]$ in anisotropic and viscous isotropic fluids shows that "microviscosity" of anisotropic fluids is an effective parameter which depends on the structure of the triplet probe (see section 4.3).

Information on the exchange interaction which modulates the hfc-induced coherent spin motion can be obtained from the magnetic field dependencies; it is well-known that B_{max}, the magnetic field strength at which $k_r(B)$ exhibits a maximum, gives a measure of the effective S−T_0 splitting energy $2J_{eff}$.[8] The effects of chain dynamics on B_{max} and hence on $2J_{eff}$ have been demonstrated by several observations. For instance, the magnetic field dependencies of the pyrene triplet yields in pyrene−$(CH_2)_n$−*N*,*N*′-dimethylaniline[33] and the $k_r(B)$ values in $^3[P^{\bullet+}-(CH_2)_6-Vi^{\bullet+}]$[19a] and $^3[P^{\bullet+}-CH_2-Ph-CH_2-Vi^{\bullet+}]$[19b] have shown the pronounced shifts of B_{max} to low fields with increasing viscosity or decreasing temperature, i.e. the slower jump frequencies result in lower $2J_{eff}$.[32−34] In the case of $^3[P^{\bullet+}-(CH_2)_6-Vi^{\bullet+}]$[19a] and $^3[P^{\bullet+}-CH_2-Ph-CH_2-Vi^{\bullet+}]$[19b] these shifts of B_{max} to low fields observed at η = 0.5−30 and 0.5−1300 cP, respectively, correlate with the enhancement of $k_r(B=0)$. The opposite effect of the jump frequencies on B_{max}[36] has been found for $^3[P^{\bullet+}-(CH_2)_n-Vi^{\bullet+}]$ in vesicular membranes (Figure 4), for $^3[P^{\bullet+}-(CH_2)_{10}-Vi^{\bullet+}]$ at η = 0.5−130 cP, and for $^3[P^{\bullet+}-(CH_2)_6-Vi^{\bullet+}]$ at η = 30−130 cP;[19a] the B_{max} values are shifted to high fields with decreasing temperature or increasing viscosity. These shifts of B_{max} to high fields correlate with the reduction of the $k_r(B=0)$ values (see Figure 4 and ref 19a), i.e. the enhancement of $2J_{eff}$ seems to be an additional factor for the retardation of the recombination of the flexible triplet RIPs in vesicular membranes and viscous isotropic fluids.

In summary, the fascinating effects of chain dynamics on the recombination of the chain-linked triplet RIPs in vesicular membranes and isotropic fluids are not simply related to the changes of the end-to-end encounter rates, but also occur through the modulation of spin dynamics by chain motions.

4.2. Solid-Fluid Phase Transitions of Vesicular Membranes. Phospholipid bilayers of the small unilamellar vesicles exhibit a rather broader thermotropic phase transition.[14] The T_m values for the transition obtained in this work (Table 1) agree with the literature values for the small unilamellar vesicles prepared by sonication.[37] For instance, the T_m values measured by the fluorescence methods[14c,40] are equal to 20.9−23.5 and 36.4−36.7 °C for DMPC and DPPC vesicles, respectively. The values of T_m obtained using probe molecules are not exactly equal to those measured by differential scanning calorimetry (T_m = 22 °C, (DMPC)[41] and 36.9 °C (DPPC)[14b]) in "pure" vesicles. The studies in many research groups[42,43] have shown that the difference in the T_m values is related to the following effects:[44] (*i*) change of T_m induced by the presence of the probe molecules in the membrane, and (*ii*) selective partitioning of the probe molecules between the solid and fluid phases. The first effect depends on the concentration of the probe molecules in membranes and usually appears in the depression of T_m.[42,43c] Although the effect of the dyad concentration on T_m was not studied in this work, analysis of the literature data[43c] showed that at the concentrations used (~0.6 mol %) the expected change of T_m did not exceed ~1 °C. The second effect has been considered by Klausner and co-workers[43b] using colligative solution theory. If γ equals the ratio of the mole fraction of lipid found in the solid phase to the mole fraction of lipid found in the fluid phase, then

$$T_m = T_0\Delta H_0/(\Delta H_0 + RT_0 \ln \gamma) \qquad (7)$$

T_m is the phase transition temperature measured in the presence

(29) The common through-space[30] and through-bonds[31] models assume exponential dependencies of J on the end-to-end distance and the number of bonds in the connecting chain.

(30) DeKanter, F.; den Hollander, J.; Huizer, A.; Kaptein, R. *Mol. Phys.* **1977**, *34*, 857.

(31) (a) McConnell, H. M. *J. Chem. Phys.* **1961**, *35*, 508. (b) Closs, G. L.; Miller, J. R. *Science* **1988**, *240*, 440.

(32) (a) Schulten, K.; Bittl, R. *J. Chem. Phys.* **1986**, *84*, 5155. (b) Bittl, R.; Schulten, K. *Chem. Phys. Lett.* **1988**, *146*, 58. (c) Bittl, R.; Schulten, K. *J. Chem. Phys.* **1989**, *90*, 1794.

(33) (a) Staerk, H.; Busmann, H.-D.; Kühnle, W.; Weller, A. *Chem. Phys. Lett.* **1989**, *155*, 603. (b) Busmann, H.-D.; Staerk, H.; Weller, A. *J. Chem. Phys.* **1989**, *91*, 4098. (c) Staerk, H.; Busmann, H.-D.; Kühnle, W.; Treichel, R. *J. Phys. Chem.* **1991**, *95*, 1906.

(34) In the theory[32] of Schulten and Bittl the end-to-end distance distribution is at equilibrium (i.e., static) and does not depend on the time scale for conformational jumps of polymethylene chains which modulate J. Hence, the effects predicted by this theory can be expected in the high-temperature and low-viscosity ranges.

(35) Olea, A. F.; Thomas, J. K. *J. Am. Chem. Soc.* **1988**, *110*, 4494.

(36) This effect is observed in viscous media, where chain motions seem to be not so fast to maintain the end-to-end distance distribution in $^3[P^{\bullet+}-(CH_2)_n-Vi^{\bullet+}]$ at equilibrium in the recombination time scale. Hence, the main postulate[34] of the theory[32] of Schulten and Bittl is not fulfilled under these conditions and further investigations are required for understanding this effect. However, these investigations were beyond the scope of this work.

(37) The phase transition parameters of the unilamellar vesicles prepared by the sonication[11] and alcohol[38] methods depend on their sizes.[39] Here, we have considered the phase transition parameters for the smallest "well" sonicated vesicles with a diameter between 200 and 300 Å.[11]

(38) Batzri, S.; Korn, E. D. *Biochim. Biophys. Acta* **1973**, *298*, 1015.

(39) (a) Takemoto, H.; Inoue, S.; Yasunaga, T.; Sukigara, M.; Toyoshima, Y. *J. Phys. Chem.* **1981**, *85*, 1032. (b) Gruenewald, B.; Stankowski, S.; Blume, A. *FEBS Lett.* **1979**, *102*, 227.

(40) Kurihara, K.; Onuki, K.; Toyoshima, Y.; Sukigara, M. *Mol. Cryst. Liq. Cryst.* **1981**, *68*, 69.

(41) Van Dijck, P. W. M.; de Kruijff, B.; Aarts, P. A. M. M.; Verkleij, A. J.; de Gier, J. *Biochim. Biophys. Acta* **1978**, *506*, 183.

(42) Albon, N.; Sturtevant, J. M. *Proc. Natl. Acad. Sci. U.S.A.* **1978**, *75*, 2258.

(43) (a) Klausner, R. D.; Wolf, D. E. *Biochemistry* **1980**, *19*, 6199. (b) Klausner, R. D.; Kleinfeld, A. M.; Hoover, R. L.; Karnovsky, M. J. *J. Biol. Chem.* **1980**, *255*, 1286. (c) Ethier, M. F.; Wolf, D. E.; Melchior, D. L. *Biochemistry* **1983**, *22*, 1178.

(44) There are other reasons for the scatter of T_m, e.g., fusion of vesicles,[45] dependence of T_m on the vesicle "age",[14b] and contaminations with large multilamellar aggregates.[14b,45b]

(45) (a) De Kruijff, B.; Cullis, P. R.; Radda, G. K. *Biochim. Biophys Acta* **1975**, *406*, 6. (b) Kantor, H. L.; Marbey, S.; Prestegard, J. H.; Sturtevant, J. M. *Biochem. Biophys. Acta* **1977**, *466*, 402.

of probe molecules, T_0 is the phase transition temperature measured without probe molecules, and ΔH_0 is the enthalpy of the phase transition. Therefore, if a probe preferentially partitions in the solid phase, the mole fraction of lipid will be higher in the fluid phase, γ will be less than 1, and T_m will be greater than T_0. The perturbations of T_m in terms of selective partitioning of the probe molecules between the solid and fluid phases depend on the spacer structure. In the DPPC vesicles (Table 1), $^3[P^{\bullet+}-CH_2-Ph-Ph-CH_2-Vi^{\bullet+}]$ with a long semirigid spacer exhibits $T_m > T_0$, whereas $^3[P^{\bullet+}-CH_2-Ph-CH_2-Vi^{\bullet+}]$ with a short semirigid spacer shows $T_m < T_0$. Hence, $^3[P^{\bullet+}-CH_2-Ph-Ph-CH_2-Vi^{\bullet+}]$ partitions into the solid phase, whereas $^3[P^{\bullet+}$-CH_2-Ph-CH_2-$Vi^{\bullet+}]$ partitions into the fluid phase. The flexible RIPs (Table 1) exhibit preferential partitioning into the solid phase because $T_m > T_0$.

The values of ΔH_{vH} obtained in this work (Table 1) also agree with those reported in the literature, e.g., Kurihara and co-workers[40] using the fluorescence intensity of *N,N'*-distearylthiacarbocyanine have obtained ΔH_{vH} values of 68.8 kcal/mol (DMPC) and 106 kcal/mol (DPPC).[46] The values of ΔH_{vH} are greater than those of ΔH_{cal} measured by differential scanning calorimetry for the small unilamellar vesicles. For instance, Suurkuusk et al.[14b] reported a value of $\Delta H_{cal} = 6.3$ kcal/mol for the DPPC vesicles. The values of $\Delta H_{cal} = 5.6$ kcal/mol (DMPC) and 7.5 kcal/mol (DPPC) have been obtained by Dijck and co-workers.[41] The difference in the ΔH_{vH} and ΔH_{cal} values usually has been explained in terms of the cooperative model of the phase transitions in phospholipid bilayers.[21] In this model a certain number of subunits (n) react simultaneously, and ΔH_{vH} is the reaction enthalpy of that portion of the system which participates in the transition. Hence, $\Delta H_{vH} = n\Delta H_{cal}$, where n is the so-called cooperative unit.[21] For the small unilamellar vesicles, the scatter in the cooperative units measured by different methods can be interpreted in terms of the lattice defects induced by the presence of impurities (e.g., probe molecules) in vesicular membranes.[42] The theoretical treatment of the effects of impurities which represent the major source of nonideality in most of the interesting biological systems has been reported by Grunewald and Stankowski.[47]

Thus, the phase transition parameters (T_m and ΔH_{vH}) of the small unilamellar vesicles extracted by the analysis of the temperature profiles of the triplet RIP recombination rates recorded in zero magnetic field are in accordance with those obtained by other spectroscopic methods.

4.3. "Microviscosity" of Fluid Vesicular Membranes. The motion of probe molecules in vesicular membranes follows Stokes type behavior, i.e. the lipid molecule diffuses or moves to create a vacancy for diffusion of the probe.[35] In terms of this model the "microviscosity" of vesicular membranes varies as the inverse of the diffusion coefficient (D). For a particle moving in a continuous medium the diffusion coefficient is given by[48]

$$D = kT/f \tag{8}$$

where k is the Boltzmann constant and f is the friction coefficient. If the dimensions of the moving molecule are large compared to those of the solvent molecules, then $f = 6\pi\eta r$ and the diffusion coefficient is given by the known Stokes–Enstein equation[48]

$$D = dT/6\pi\eta r \tag{9}$$

where r is the radius of the moving molecule.[49] Equation 9 gives a possible method for estimating the "microviscosity" of vesicular membranes from the values of D measured by the other kinetic methods. For instance, the value of η calculated from the values of D for excimer formation of pyrene in DPPC bilayers[50] decreases from 67 to 38 cP in the range of 45–60 °C and the corresponding activation energy of viscous flow $W_\eta = 8.8$ kcal/mol. The "microviscosity" of the DPPC vesicular membranes estimated by eq 9 from the values of D reported by Kano and co-workers[4a] for the fluorescence quenching of pyrene derivatives by aromatic amines varies in the range of 17–25 cP (50 °C) depending on the probe molecule. The difference in the η values measured by different methods can be related to the limits of the Stokes–Einstein relationship[22,35] for calculation of membrane "microviscosity".

The effect of the spacer length on the η values measured using $^3[P^{\bullet+}-(CH_2)_n-Vi^{\bullet+}]$ as a probe (Figure 5) can be explained in terms of the "microviscosity" changes in the transversal membrane plane. In vesicular membranes formation of $^3[P^{\bullet+}-(CH_2)_n-Vi^{\bullet+}]$ is expected to occur via the end-to-end encounters of the hydrophobic porphyrin located within the lipid alkyl chains and the hydrophilic viologen anchored near the lipid headgroup–water interface. After the electron transfer reaction the porphyrin acquires a positive charge and becomes more hydrophilic. Nevertheless, the porphyrin radical cation can penetrate into the membrane. Dannhauser and co-workers[51] have shown that an oxidized manganese porphyrin (i.e. porphyrin with a positive charge) penetrates vesicular membranes to a depth limited by the hydrocarbon spacer linking it to the extremely hydrophilic polymer. Hence, the smaller η values for $^3[P^{\bullet+}-(CH_2)_{10}-Vi^{\bullet+}]$ can show that "microviscosity" of vesicular membranes decreases with the distance from the lipid headgroup–water interface.[52]

In summary, the "microviscosity" of the fluid vesicular membranes calculated from the recombination rates of flexible triplet RIPs in the fluid bilayers and in methanol/glycerol mixtures with known viscosity is compared with that obtained from the rates of the diffusion-controlled reactions. The recombination of the flexible triplet RIPs provides for detecting the membrane "microviscosity" not only at different temperatures but also at different distances from the lipid headgroup–water interface.

5. Conclusions

Through a systematic variation of the connecting chain structure and detailed analysis of the kinetic data we have extended using the magnetic-field-sensitive recombination of the chain-linked triplet radical ion pairs from a simple probing of the phase transitions up to detecting the phase transition parameters and particularly the "microviscosity" of the vesicular

(46) $\Delta H_{vH} = 120-130$ kcal/mol for the small unilamellar vesicles can be estimated from the dependence of ΔH_{vH} on the vesicle size (see Figure 9 in ref 39a).

(47) Gruenewald, B.; Stankowski, S. *Biophys. Chem.* **1980**, *12*, 167.

(48) (a) Noyes, R. M. *Prog. React. Kinet.* **1961**, *1*, 129. (b) Rice, S. A. In *Comprehensive Chemical Kinetics*; Bamford, C. H., Compton, R. G., Eds.; Elsivier: New York, 1985; Vol. 25.

(49) The calculation of D from eq 9 is a crude approximation only, because the probe molecule is not a sphere of radius r, moving in a continuum of viscosity. The limitations of eq 9 in predicting the values of D have been given in many studies.[22,35]

(50) Galla, H.-J.; Sackmann, E. *Biochem. Biophys. Acta* **1974**, *339*, 103.

(51) (a) Nango, M.; Dannhauser, T.; Huang, D.; Spears, K.; Morrison, L.; Loach, P. *Macromolecules* **1984**, *17*, 1898. (b) Dannhauser, T. J.; Nango, M.; Oku, N.; Anzai, K.; Loach, P. A. *J. Am. Chem. Soc.* **1986**, *108*, 5865.

(52) Viologen radical cation is more hydrophobic than viologen and also can penetrate into the membranes.[53] Hence, the actual dynamics of $^3[P^{\bullet+}-Sp-Vi^{\bullet+}]$ in vesicular membranes seems to be more complex and can include the transversal movements of both the porphyrin and viologen radical cations.

(53) For recent reviews, see: Hurst, J. K. *Kinetics and Catalysis in Microheterogeneous Systems*; Marcel Dekker: New York, 1991; Surfactant Science Series, Vol. 38, pp 183–226.

membranes. The interplay of the results of this work and extensive literature extracts have shown that the temperature and van't Hoff enthalpy of the phase transition and the "microviscosity" of the vesicular membranes detected by the chain-linked triplet radical ion pairs are compared with those values obtained using other techniques. The most intriguing benefit of using the chain-linked triplet radical ion pairs as probes of membrane dynamics is that information on their chain motions can be obtained from not only the temperature profiles of the recombination rates but also from the magnetic field dependences.

Acknowledgment. The authors thank Dr. I. V. Khydyakov for many helpful discussions.

Supplementary Material Available: Table of $k_{rs}°$, $k_{rf}°$, $k_r°(B=0.21T)$, and $\eta°$ values (1 page). This material is contained in many libraries on microfiche, immediately follows this article in the microfilm version of the journal, can be ordered from the ACS, and can be downloaded from the Internet; see any current masthead page for ordering information and Internet access instructions.

JA943597P